

1 Topological constraints in early 2 multicellularity favor reproductive 3 division of labor

4 David Yanni^{a*}, Shane Jacobeen^{a*}, Pedro Márquez-Zacarías^{b,c}, Joshua S. Weitz^{a,c},
5 William C. Ratcliff^{c, 1}, Peter J. Yunker^{a, 2}

***For correspondence:**

6 william.ratcliff@biology.gatech.edu (WCR);
7 peter.yunker@physics.gatech.edu (PJY)

8 †These authors contributed equally
9 to this work

10 ‡These authors also contributed
equally to this work

6 ^aSchool of Physics, Georgia Institute of Technology, North Ave NW, Atlanta, GA 30332;
7 ^bInterdisciplinary Graduate Program in Quantitative Biosciences, Georgia Institute of
8 Technology; ^cSchool of Biological Sciences, Georgia Institute of Technology, North Ave NW,
Atlanta, GA 30332

11 **Abstract** Reproductive division of labor (e.g., germ-soma specialization) is a hallmark of the
12 evolution of multicellularity, signifying the emergence of a new type of individual and facilitating the
13 evolution of increased organismal complexity. A large body of work from evolutionary biology,
14 economics, and ecology has shown that specialization is beneficial when further division of labor
15 produces an accelerating increase in absolute productivity (i.e., productivity is a convex function of
16 specialization). Here we show that reproductive specialization is qualitatively different from
17 classical models of resource sharing, and can evolve even when the benefits of specialization are
18 saturating (i.e., productivity is a concave function of specialization). Through analytical theory and
19 evolutionary individual-based simulations, we demonstrate that reproductive specialization is
20 strongly favored in sparse networks of cellular interactions that reflect the morphology of early,
21 simple multicellular organisms, highlighting the importance of restricted social interactions in the
22 evolution of reproductive specialization.

24 Introduction

25 The evolution of multicellularity set the stage for unprecedented increases in organismal complexity
26 *Szathmáry and Smith (1995); Knoll (2011)*. A key factor in the remarkable success of multicellular
27 strategies is the ability to take advantage of within-organism specialization through cellular differen-
28 tiation *Queller and Strassmann (2009); Brunet and King (2017); Cavalier-Smith (2017)*. Reproduc-
29 tive specialization, which includes both the creation of a specialized germ line during ontogeny
30 (as in animals and volvocine green algae) and functional differentiation into reproductive and
31 non-reproductive tissues (as in plants, green and red macroalgae, and fungi), may be especially
32 important *Cooper and West (2018); Michod et al. (2006); Ispolatov et al. (2012); Solari et al. (2013);*
33 *Michod (2007); West et al. (2015)*. Reproductive specialization is an unambiguous indication that
34 biological individuality rests firmly at the level of the multicellular organism *Michod (1999); False III*
35 *and Roughgarden (2010)*, and is thought to play an important role in spurring the evolution of
36 further complexity by inhibiting within-organism (cell-level) evolution *Buss (1988)* and limiting re-
37 version to unicellularity *Libby and Ratcliff (2014)*. Despite the central importance of reproductive
38 specialization, its origin and further evolution during the transition to multicellularity remain poorly
39 understood *McShea (2000)*.

40 The origin of specialization has long been of interest to evolutionary biologists, ecologists, and

41 economists. A large body of theory from these fields shows that specialization pays off only when it
 42 increases total productivity, compared to the case where each individual simply produces what they
 43 need *Szathmáry and Smith (1995); Smith and Szathmáry (1997); Goldsby et al. (2012); Corning*
 44 *and Szathmáry (2015); Hidalgo and Hausmann (2009); Boza et al. (2014); Taborsky et al. (2016);*
 45 *Page et al. (2006); Rueffler et al. (2012); Szekely et al. (2013); Findlay (2008); Amado et al. (2018).*
 46 Certain types of trading arrangements maximize the benefits of specialization; highly reciprocal
 47 interactions, which facilitate exchange between complementary specialists, amplify cooperation
 48 *Allen et al. (2017); Pavlogiannis et al. (2018).* Still, previous work finds that even when groups
 49 grow in an ideal spatial arrangement, increased specialization and trade is only favored by natural
 50 selection when productivity increases as an accelerating function of the degree of specialization
 51 (i.e., productivity is a convex, or super-linear, function of the degree of specialization). Conversely,
 52 saturating functional returns (i.e., productivity is a concave, or sub-linear, function of the degree of
 53 specialization) should inhibit the evolution of specialization *Cooper and West (2018); Michod et al.*
 54 *(2006); Ispolatov et al. (2012); Solari et al. (2013); Michod (2007); West et al. (2015).*

55 Reproductive specialization differs from classical models of trade in several key respects. Trade
 56 between germ (reproductive) and somatic (non-reproductive) cells is intrinsically asymmetric,
 57 because the cooperative action, multicellular replication, is not a product that is shared evenly. Se-
 58 lection acts primarily on the fitness of the multicellular group as a whole *Folse III and Roughgarden*
 59 *(2010)*. As a result, optimal specialization can result in behaviors that reduce the short-term fitness
 60 of some cells within the multicellular group *Michod et al. (2006); Michod (2007)*, often manifest as
 61 reproductive altruism.

62 Understanding the evolution of cell-cell trade, a classic form of social evolution *Kirk (2005a)*,
 63 requires understanding the extent of between-cell interactions. Network theory has proven to be
 64 an exceptionally powerful and versatile technique for analyzing social dynamics *Wey et al. (2008);*
 65 *Lieberman et al. (2005)*, and indeed, is uniquely well suited to understanding the evolution of early
 66 multicellular organisms. When cells adhere through permanent bonds, sparse network-like bodies
 67 (i.e., filaments and trees) often result *Amado et al. (2018)*. This mode of group formation is not only
 68 common today among simple multicellular organisms (*Umen (2014); Claessen et al. (2014)*), but is
 69 the dominant mode of group formation in the lineages evolving complex multicellularity (i.e., plants,
 70 red algae, brown algae, and fungi, but not animals).

71 In this paper, we develop and investigate a model for how the network topology of early multisel-
 72 lular organisms affects the evolution of reproductive specialization. We find that under a broad class
 73 of sparse networks, complete functional specialization can be adaptive even when returns from
 74 dividing labor are saturating (i.e., concave / sub-linear). Sparse networks impose constraints on who
 75 can share with whom, which counterintuitively increases the benefit of specialization *McShea (2000)*.
 76 By dividing labor, multicellular groups can capitalize on high between-cell variance in behavior,
 77 ultimately increasing group-level reproduction. Further, we consider group morphologies that
 78 naturally arise from simple biophysical mechanisms and show that these morphologies strongly
 79 promote reproductive specialization. Our results show that reproductive specialization can evolve
 80 under a far broader set of conditions than previously thought, lowering a key barrier to major
 81 evolutionary transitions.

82 Model

83 Reproductive specialization can be modeled as the separation of two key fitness parameters,
 84 those related to either viability or fecundity, into separate cells within the multicellular organism
 85 *Michod (2005); Folse III and Roughgarden (2010)*. The dichotomy of viability versus fecundity was
 86 originally used by Michod *Michod (2005)* to partition components of cellular fitness into actions
 87 that contribute to keeping a cell alive (viability), and actions that directly contribute to reproduction
 88 (fecundity). Multicellular organisms often have evolved to divide labor along these two lines (i.e.,
 89 reproduction by germ cells and survival provided by somatic cells), while their unicellular ancestors
 90 had to do both. We define viability as activities keeping the cell alive (e.g., investing in cellular

91 homeostasis or behaviors that improve survival), and fecundity as activities involved in cellular
92 reproduction.

93 At the cellular level, there appears to be a fundamental asymmetry in how viability effort
94 and fecundity effort can be shared among cells: while multicellular organisms readily evolve
95 differentiated cells that are completely reliant on helper cells (i.e., glial cells that support neurons
96 in animals or companion cells that support sieve tube cells in plants), no cell can directly share its
97 ability to reproduce. To better understand the intuition behind this, consider a cell that elongates
98 prior to fission. This cell must grow to approximately twice its original length. Two cells cannot
99 elongate by 50% and then combine their efforts; elongation is an intrinsically single cell effort. We
100 thus use a model in which viability can be shared across connected cells, but fecundity cannot
101 be shared (note, in a later section we will consider the more general case in which viability and
102 fecundity can both be shared, but by different amounts).

103 We consider a model of multicellular groups composed of clonal cells that each invest resources
104 into viability and fecundity. Because there is no within-group genetic variation, within-group
105 evolution is not possible, though selection can act on group-level fitness differences. Specifically,
106 we consider the pattern of cellular investment in fecundity and viability, and their sharing of these
107 resources with neighboring cells within the group, to be the result of a heritable developmental
108 program. Thus, selection is able to act on the multicellular fitness consequences of different
109 patterns of cellular behavior within the group. We let v denote each cell's investment into viability,
110 and b denote each cell's investment into fecundity. Each cell's total investment is constrained so
111 that $v + b = 1$. However, a cell's return on its investment is in general nonlinear. Here, we let α
112 represent the 'return on investment exponent': by tuning α above and below 1.0, we can simulate
113 conditions with accelerating and saturating (i.e., convex and concave, or super- and sub-linear)
114 returns on investment, respectively. We let \tilde{v} and \tilde{b} represent a cell's return on viability and fecundity
115 investments, respectively. Following Michod *Michod (2005); Michod and Roze (1997)*, we calculate
116 a cell's reproductive output as a multiplicative function of \tilde{v} and \tilde{b} (thus, both functions must be
117 positive for a cell to grow). A single cell's reproduction rate is $w = \tilde{v}\tilde{b} = v^\alpha b^\alpha$. At the group level,
118 fitness is the total contribution of all cells in the group toward the production of new groups (i.e.
119 group level reproduction). The group level fitness is thus the sum of $\tilde{v}\tilde{b}$ over all cells.

120 Finally, cells may share the products of their investment in viability with other cells to whom
121 they are connected. For a given group, the details about who may share with whom, and how much,
122 is encoded in a weighted adjacency matrix \mathbf{c} . The element c_{ij} defines what proportion of viability
123 returns cell i shares with cell j . Cells cannot give away all of their viability returns, as they would no
124 longer be viable; mathematically, we count a cell among its neighbors and thus ensure that they
125 always "share" a positive portion of viability returns with themselves, so that $c_{ii} > 0$. Furthermore,
126 since a cell cannot share more viability returns than the total it possesses, we have $\sum_{i=1}^N c_{ji} = 1$ for a
127 group of N cells. For the networks we consider, each cell takes a fraction β of its viability returns
128 and shares that fraction equally among all of its n_i neighbors (including itself), and keeps the rest of
129 its returns $1 - \beta$ for itself. Therefore cell i keeps a total fraction of $1 - \beta + \frac{\beta}{n_i}$ of its returns for itself
130 and gives $\frac{\beta}{n_i}$ to each of its non-self neighbors. In other words, $c_{ii} = 1 - \beta$, $c_{ij} = \frac{\beta}{n_i}$ if cells i and j are
131 connected, and $c_{ij} = 0$ if cells i and j are not connected. This means the total amount of returns
132 kept by cell i depends on *both* the network topology and β . When $\beta = 0$ there is no sharing, and
133 when $\beta = 1$ cells share everything equally among all connections and themselves. We refer to β
134 as interaction strength. A given group topology (unweighted adjacency matrix) and β completely
135 specify \mathbf{c} .

136 Within a group of N cells, the overall returns on viability that a given cell enjoys, then, comprises
137 its own returns as well as whatever is shared with it by other members of the group. This can be
138 written as $\tilde{v}_i = v_i^\alpha c_{ii} + \sum_{j \neq i} v_j^\alpha c_{ji}$, or equivalently, $\tilde{v}_i = \sum_j v_j^\alpha c_{ji}$. Note that this is a column sum, since it
139 describes the total *incoming* viability returns a cell receives as a result of its own effort and trade
140 with neighboring cells. Therefore, we write the group level reproduction rate (i.e., the group fitness)

141 for a group of N cells as

$$\begin{aligned}
 W &= \sum_{i=1}^{i=N} \tilde{b}_i \cdot \tilde{v}_i \\
 W &= \sum_{i=1}^{i=N} \tilde{b}_i \sum_{j=1}^{j=N} v_j^\alpha c_{ji} \\
 W &= \sum_{i=1}^{i=N} \sum_{j=1}^{j=N} b_i^\alpha c_{ji} v_j^\alpha, \tag{1}
 \end{aligned}$$

143 where all three of the above equations are equivalent. We investigate evolutionary outcomes under
 144 this definition of group level fitness for groups with different topologies (who shares with whom),
 145 and in scenarios with various return on investment exponents α .

146 Results

147 Fixed resource sharing

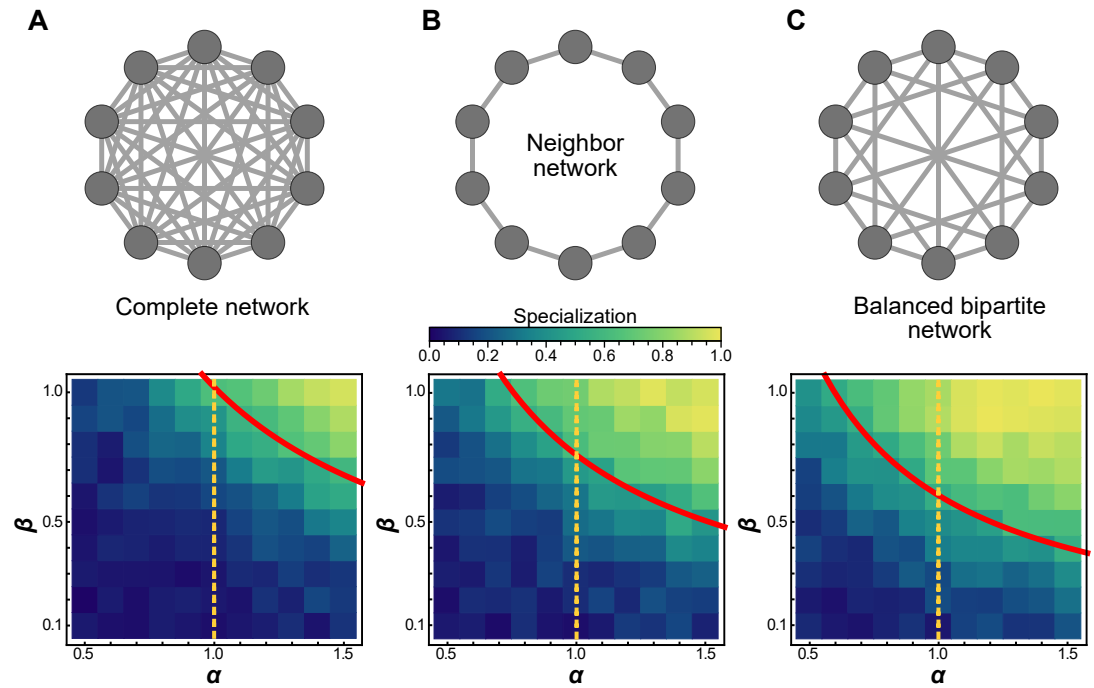


Figure 1. Schematic of topology for a simplified six cell group (first row), and mean specialization as a function of specialization power α and interaction strength β across the entire population. (a) When each cell in the group is connected to all others, specialization is favored only when $\alpha > 1$. (b) For the nearest neighbor topology, specialization is favorable for a wider range of parameters, including for some values of $\alpha < 1$. Specifically, specialization is advantageous when $\alpha > \frac{3}{4\beta}$. (c) Connecting alternating specialists creates a bipartite graph which maximizes the benefits of specialization and the range of parameters for which it is advantageous. In this case specialization is favorable wherever $\alpha > \frac{3}{5\beta}$. The red curves represent analytical predictions for α^* , the lowest value of α for which complete generalization is disfavored, and the orange vertical lines are at $\alpha = 1$ to guide the eye. While analysis shows that *some* degree of specialization must occur in the regime upward and to the right of the red curves, simulations reveal that when complete generalization is disfavored complete specialization *is* favored in these networks.

148 We first consider cases wherein cells within a group share across fixed intercellular interactions.
 149 In each case we vary the return on investment exponent, α , between 0.5 and 1.5, and the interaction

150 strength, β , between 0.0 and 1.0, both in increments of 0.1. For each combination of topology, α ,
 151 and β , the group investment strategy (v_i for all i) was allowed to evolve for 1000 generations.

152 We begin with simple topologies: groups with no connections and groups that are maximally
 153 connected. They represent, respectively, the case in which all cells within the group are autonomous
 154 and the case in which every cell interacts with all others (i.e., a ‘well-mixed’ group). In the absence of
 155 interactions, cells cannot benefit from functions performed by others and therefore must perform
 156 both functions v and b ; hence specialization is not favored, and does not evolve. In the fully
 157 connected case, a high degree of specialization is observed for many values of α and β (Figure
 158 1a). Consistent with classic results *Cooper and West (2018)*; *Michod et al. (2006)*; *Ispolatov et al.*
 159 *(2012)*; *Solari et al. (2013)*; *Michod (2007)*; *West et al. (2015)*, specialization is only achieved in the
 160 fully connected case for $\alpha > 1$.

161 Next, we consider a simple sparse network in which each cell within a group is connected
 162 to only two other cells, forming a complete ring (Figure 1b); we refer to this as the neighbor
 163 network. Surprisingly, preventing trade between most cells encourages division of labor. We
 164 find that specialization evolves even when $\alpha < 1.0$, i.e., when the returns on investment are
 165 saturating or concave. In our simulations, this topology leads to alternating specialists in viability
 166 and fecundity (Figure 1b). Analytically, we find that this topology always favors at least some degree
 167 of specialization whenever $\alpha > \frac{3}{4\beta}$.

168 We next study a network with cells that can be separated into two disjoint sub-groups, where
 169 every edge of the network connects a cell in one sub-group to a cell in the other sub-group and
 170 no within sub-group connections exist, i.e., a bipartite graph (Figure 1c). We refer to the specific
 171 network structure in Figure 1c as the ‘balanced bipartite’ network. We find that specialization
 172 evolves even when $\alpha < 1.0$, similar to the neighbor network. However, we find that specialization
 173 evolves for a wider range of α and β values for the balanced bipartite network than for the neighbor
 174 network.

175 We can analytically determine under what conditions complete generalization is optimal. The
 176 complete generalist investment strategy is where every cell in the group invests equally into viability
 177 and fecundity, defined as: $v_i^* = \frac{1}{2}$ for all i . For these simple topologies the complete generalist
 178 strategy is either a maximum or a saddle point, depending on the values of α and β . Complete
 179 generalization is only favored when the Hessian evaluated at the generalist investment strategy
 180 $\left. \frac{\partial^2 W}{\partial v_k \partial v_\ell} \right|_{\vec{v}^*} = \mathbf{H}^*$ is negative definite, i.e. all of its eigenvalues are negative. The largest eigenvalues of
 181 the Hessian for the complete, neighbor, and balanced bipartite networks are $\alpha \left(\frac{1}{2}\right)^{2\alpha-3} (-1 + \alpha\beta)$,
 182 $\alpha \left(\frac{1}{2}\right)^{2\alpha-3} (-1 + \frac{4}{3}\alpha\beta)$, and $\alpha \left(\frac{1}{2}\right)^{2\alpha-3} (-1 + \frac{2N}{N+2}\alpha\beta)$, respectively. When α and β are chosen so that the
 183 largest eigenvalue becomes non-negative, complete generalization cannot maximize group fitness.

184 While we have not analytically shown where the fitness maximum occurs in cases where the
 185 generalist strategy becomes a saddle point, evolutionary simulations (Figure 1) suggest that when
 186 complete generalization is not a fitness maximum, a high degree of (or even complete) specialization
 187 typically *does* maximize fitness.

188 In all cases in which complete specialization is achieved in evolutionary simulations, $\vec{v}\vec{b}$ terms for
 189 viability specialists go to zero, as they cannot reproduce on their own. Furthermore, the fecundity
 190 specialists are entirely reliant on the viability specialists for their survival; if viability sharing were
 191 suddenly prevented, their $\vec{v}\vec{b}$ terms would also be zero. This amounts to complete reproductive
 192 specialization *Cooper and West (2018)*; *Kirk (2005a)*; *Michod (2005)*.

193 **Evolving resource sharing**

194 Until now, sharing has been included in every intercellular interaction within groups. Here, we
 195 consider the case in which there is initially no sharing, and sharing must evolve along with special-
 196 ization. These simulations begin with no resource sharing (i.e., $\beta = 0$); during every round, each
 197 group in the population has a 2% chance that a mutation will impact its developmental program,
 198 and the β value for one of its cells will change. The new β value is chosen from a truncated Gaussian

199 with standard deviation of 10% of the mean, centered on the current value. Whatever is not retained
 200 is shared equally across all interactions, including the self term.

201 Evolutionary simulation results are similar to those from the fixed-sharing model (Supplemental
 202 Figure 1). Saturating specialization (i.e., specialization despite a concave return function) still occurs
 203 for the neighbor and balanced bipartite topologies. Thus, for both fixed and evolved resource
 204 sharing, we observe specialization for the largest range of parameters (including $\alpha < 1$) not when
 205 the group is maximally connected, but rather when connections are fairly sparse. Therefore, a
 206 sparse group topology readily constitutes a cooperation-prone physical substrate that can sustain
 207 evolvability of specialization traits.

208 As an example of the benefit of evolving sharing, consider that the maximum fitness according
 209 to eq. 1 for a group of N disconnected cells scales as $N \left(\frac{1}{2}\right)^{2\alpha}$. On the other hand, for the balanced
 210 bipartite network with a complete specialization strategy (i.e. $\vec{v} = \langle 0, 1, 0, 1, \dots \rangle$), the fitness scales as
 211 $\left(\frac{N^2\beta}{2N+2}\right)$. The ratio of these fitnesses is $\left(\frac{N^2\beta}{2N+2}\right) 2^{2\alpha} \approx \beta 2^{2\alpha-1}$, where the approximation is for large N .
 212 So for larger groups and when $\alpha > \frac{1}{2} - \frac{\log \beta}{2 \log 2}$, if a group can evolve resource sharing (i.e. letting $\beta \rightarrow 1$
 213 and adopting the specialist investment strategy) its maximum fitness will increase.

214 **Benefit of specialization**

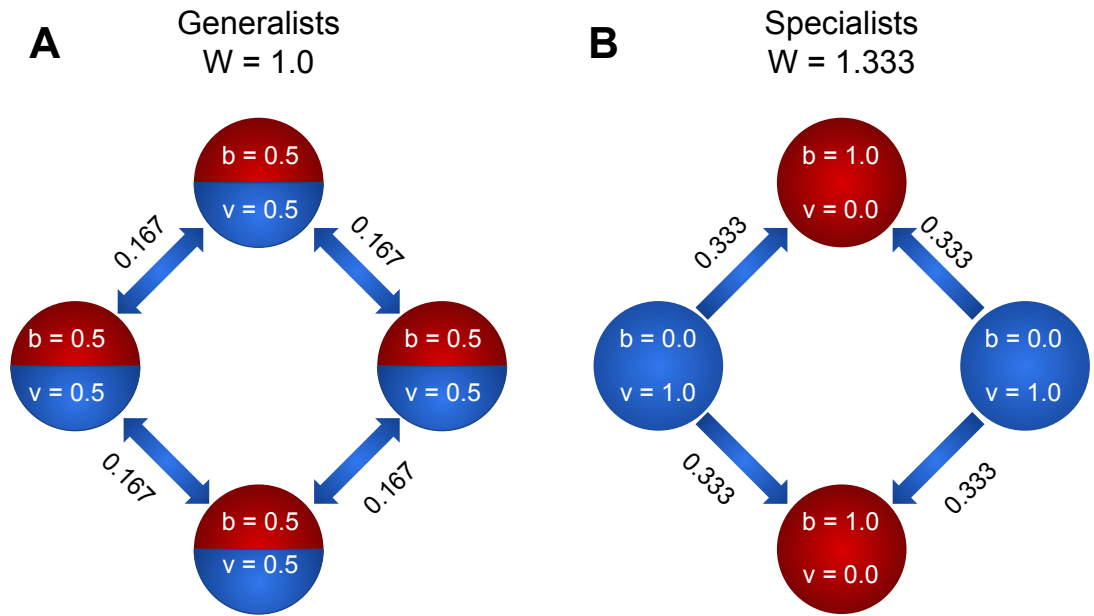


Figure 2. To explore how specialization can be favored by the nearest-neighbor topology, we compare the fitness of a four member system when cells are (a) generalists and (b) specialists. We first consider the case of linear functional returns ($\alpha = 1$). For the case of generalists (a), each cell receives as much viability as it shares, and all nodes contribute equally to the fitness of the group. Therefore, the fitness of the group is $W = 4 \cdot \frac{1}{2} \cdot \frac{1}{2} = 1$. For the case of specialists, however, the viability specialist cells (blue) have $\vec{v}\vec{b} = 0$, while the fecundity specialist cells have nonzero $\vec{v}\vec{b}$ due to the fact that they receive $\frac{1}{3}$ of each viability specialist's output. Thus the fitness of the group is $W = 2(2 \cdot \frac{1}{3}) = \frac{4}{3}$. Thus fitness is higher for the group of specialists, so specialization is favored. For $\alpha = 0.9$, the fitness of generalists is 1.15, and the fitness of specialists is 1.33. Thus, even though the returns on investment are saturating (i.e., concave), specialization is favored.

215 We now consider a simple example to highlight why specialization can be adaptive despite
 216 saturating (i.e., concave) returns from trade. Consider groups of four cells, connected via the
 217 nearest-neighbor topology (i.e., in a ring). We directly calculate the group-level fitness of generalists
 218 and specialists for two scenarios: $\alpha = 0.9$ and $\alpha = 1$ by summing the contributions of each cell within
 219 these groups (Figure 2). In this simple scenario, reproductive specialization strongly increases group

220 fitness (33% for $\alpha = 1$ and 16% for $\alpha = 0.9$).

221 The benefit of specialization in neighbor networks increases with group size. For a ring of size
 222 N , fitness under the specialist strategy $\vec{v} = \langle 0, 1, 0, 1, \dots \rangle$ is $W = \frac{\beta}{3}N$. For a ring of generalists the
 223 fitness is $W = N(\frac{1}{2})^{2\alpha}$. Therefore, whenever $\alpha > \frac{\log 3 - \log \beta}{2 \log 2}$, the ring of complete specialists enjoys
 224 a greater fitness than the ring of complete generalists. Again, note that complete generalization
 225 becomes disfavored when $\alpha > \frac{3}{4\beta}$, so there is a narrow regime where $\frac{3}{4\beta} < \alpha < \frac{\log 3 - \log \beta}{2 \log 2}$ during which
 226 neither complete generalization nor complete specialization is optimal. Numerical optimization
 227 and evolutionary simulations suggest that even in this region, however, the specialization score of
 228 the optimal strategy is large (Figure 1).

229 Effect of sparsity

230 Surprisingly, saturating specialization appears to be the rule, rather than the exception, for sparsely
 231 connected graphs. We investigated Erdős-Rényi random graphs with varying degrees of connect-
 232 ivity to systematically examine the relationship between sparsity and the value of α at which
 233 specialization is favored. We find that many randomly assembled graphs obtain maximum fitness
 234 through complete reproductive specialization even when α is below 1 (Figure 3 b,c). It is only at the
 235 extremes of sparsity and connectivity (near the fully connected or fully unconnected points) that
 236 generalists maintain superior fitness for all values of $\alpha < 1$. We further show that this general trend
 237 is independent of the size of a group; saturating specialization is favorable for groups of size $N = 10$,
 238 $N = 100$, and $N = 1000$. When network connectivity is at its minimum, the group consists solely
 239 of isolated cells that cannot interact. Under these conditions generalists are favored. Similarly, at
 240 maximum connectivity every cell interacts with every other cell. Under these conditions generalists
 241 are favored unless $\alpha\beta > 1$. However, when connectivity is small but not zero, specialization arises
 242 most readily. We conjecture that the troughs in Figure 3 b, where specialization occurs for the
 243 lowest values of α , occur when connectivity is just large enough so that the existence of a spanning
 244 tree is more likely than not.

245 Filaments and trees

246 Sparse topologies like the neighbor network configuration have significant biological relevance, and
 247 direct ties to early multicellularity. The first step in the evolution of multicellularity is the formation
 248 of groups of cells *Szathmáry and Smith (1995); Kirk (2005b); Willensdorfer (2008); Bonner (1998);*
 249 *Fairclough et al. (2010)*. Simple groups readily arise through incomplete cell division, forming either
 250 simple filaments (Figure 4a) or tree-like morphologies (Figure 4b) *Bengtson et al. (2017b); Droser*
 251 *and Gehling (2008); Berman-Frank et al. (2007); Ratcliff et al. (2012)*. Filament topologies have been
 252 widely observed in independently-evolved simple multicellular organisms, from ancient fossils of
 253 early red algae *Butterfield (2000b)*(Figure 4a) to extant multicellular bacteria *Claessen et al. (2014)*
 254 and algae *Umen (2014)*. Branching multicellular phenotypes have also been observed to readily
 255 evolve from baker's yeast *Ratcliff et al. (2015)*(Figure 4b), and are reminiscent of ancient fungus-like
 256 structures *Bengtson et al. (2017a)* and early multicellular fossils of unknown phylogenetic position
 257 from the early Ediacaran *Droser and Gehling (2008)*.

258 Simulations of populations of groups with filamentous and branched topologies reveal that
 259 specialization is indeed favored in the sub-linear regime (Figure 4a and 4b). While the generalist
 260 strategy is never a critical point for these networks (which have $\mathbf{c} \neq \mathbf{c}^T$, see methods), we conjecture
 261 that there is a nearby critical point which maximizes fitness at small values of α and becomes
 262 unstable at larger values of α . We introduce a new metric, α^* , defined as the value of α such that
 263 the largest (least negative) eigenvalue of the Hessian evaluated at the complete generalist strategy
 264 is zero when $\beta = 1$. For topologies in which each member has the same number of neighbors,
 265 α^* is a critical value at which generalization is no longer an optimal strategy. However, even for
 266 groups where the number of neighbors for each cell varies, we can still use α^* as a proxy for how
 267 amenable a topology is to saturating specialization. The smaller α^* , the more specialization is likely
 268 to be favored. We plot vertical lines where $\alpha = \alpha^*$ (solid green fig 4(a) and blue fig 4(b)), and dotted

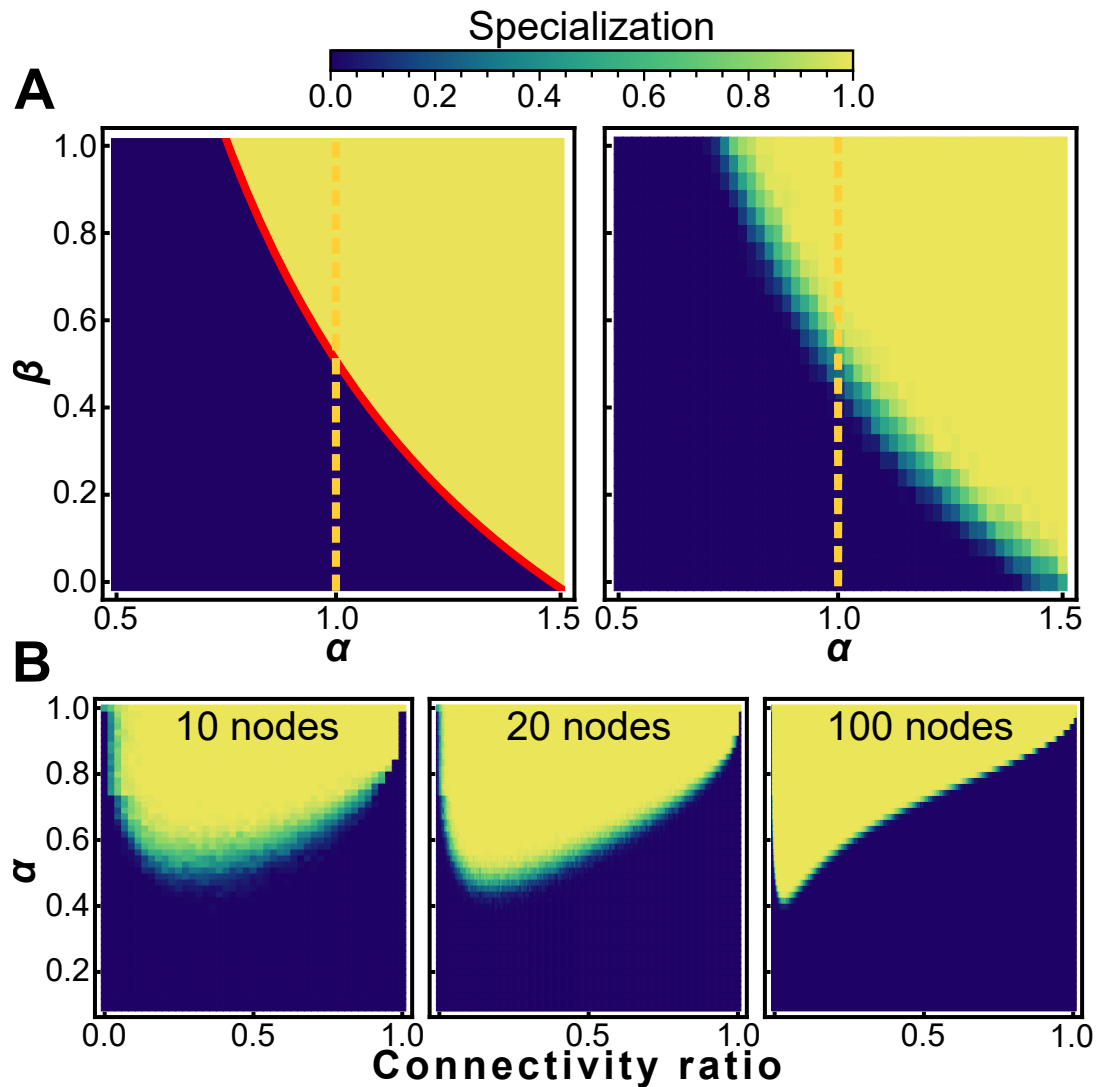


Figure 3. Sparsity encourages specialization. Heat maps showing conditions that favor specialists (white) and generalists (black) for nearest neighbor topologies (A, left) and randomly generated graphs with the same connectivity as nearest neighbor topologies (A, right). Specialization is adaptive on a neighbor network for $\alpha > \frac{3}{4\beta}$; random networks with the same mean connectivity as the nearest neighbor topology behave similarly. (B) The sparsity of a random graph affects how likely it is to favor specialization. We numerically maximize fitness for random graphs of size $N = 10$ (left), $N = 20$ (middle), and $N = 100$ (right) at different levels of sparsity, and subsequently measure the specialization S of the fitness maximizing investment strategy. The horizontal axis is the fraction of possible connections present ranging from 0 (none) to 1 (all). The vertical axis is the specialization power α , and the colormap shows mean specialization.

269 lines to indicate roughly where the simulation curves cross specialization of 0.5. These results
 270 show that, for these topologies, α^* acts as an effective metric for how amenable a network is to
 271 saturating specialization. This metric α^* only depends on topology and can in principle be calculated
 272 analytically given any network. We examined the value of α^* as filaments and a variety of tree-like
 273 structures grow larger, and find that specialization becomes more strongly favored (Figure 4c).
 274 While group size has no effect on specialization for some topologies, like the neighbor network,
 275 filaments and trees all see a decrease in α^* as group size increases; α^* eventually plateaus once
 276 groups are larger than a few tens of cells. Simple and easily accessible routes to multicellular group
 277 formation can readily evolve in response to selection for organismal size *Ratcliff et al. (2012)*, and
 278 this process may also strongly favor the evolution of cellular differentiation *McCarthy and Enquist*

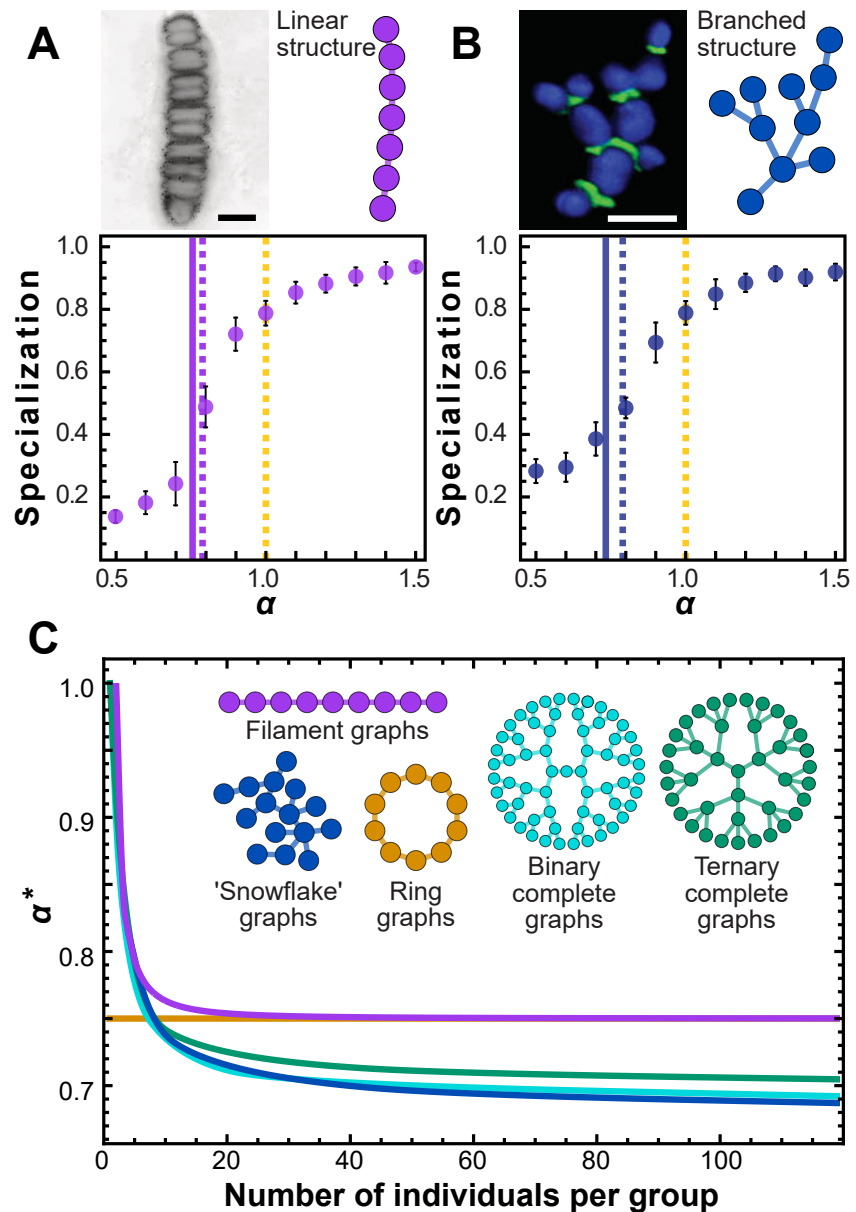


Figure 4. Simple multicellular organisms with sparse topologies. We show two examples of simple multicellular organisms with linear and branched topologies. The image in (a) is a fossilized rhodophyte specimen of *Bangiomorpha pubescens*, courtesy of Prof. Nicholas Butterfield (see e.g. [Butterfield \(2000a\)](#)); Prof. Butterfield has granted permission to distribute this image under the terms of a Creative Commons Attribution license (<https://creativecommons.org/licenses/by/4.0/>); further reproduction of this image should adhere to the terms of the CC BY 4.0 license with an attribution to Prof. Butterfield; the image in (b) is a confocal image of 'snowflake yeast' showing cell volumes in blue and cell-cell connections in green. Scale bars in both panels = $10\mu\text{m}$. Panels include cartoons depicting simplified topologies. Topologically similar to the two-neighbor configuration, these configurations yield similar simulation results. Specialization is plotted as a function of α . Solid green (a) and blue (b) vertical lines indicate analytical solutions for the transition point where the Hessian evaluated at $\vec{v} = \frac{1}{2}\vec{1}$ stops being negative definite, i.e. α^* ; dotted lines indicate roughly where the simulation curves cross specialization of 0.5, i.e. the "true" transition value of α where specialization becomes favored. (c) To further explore trees and filaments we analytically solved for α^* for various types of trees and filaments of different sizes. α^* is plotted versus group size for several topologies. This is a proxy measure of how amenable a network structure is to specialization.

279 (2005); Heim et al. (2017); McClain and Boyer (2009); Bonner (1998).

280 Mean field model

281 Finally, to capture some general principles underlying this phenomenon, we consider a mean-field
 282 model with N cells, each of which is connected to z other cells. For simplicity we consider the case
 283 in which $\beta = 1$ and $\alpha = 1$. We pick $\alpha = 1$ as at this point, if the fitness of specialists is greater than
 284 that of generalists, specialization will be favored for at least some values of $\alpha < 1$. If the fitness of
 285 generalists is greater than or equal to that of specialists, specialization will only be favored if $\alpha > 1$.

286 For generalists, the fitness is simply $W_G = N/4$, as each cell has $v = 1/2$ and $b = 1/2$ (before
 287 and after sharing). Viability specialists produce $v = 1$ and $b = 0$, while fecundity specialists produce
 288 $v = 0$ and $b = 1$. Viability specialists then share $v = 1/(z + 1)$ with each of their z neighbors. After
 289 sharing, fecundity specialists receive $v = 1/(z + 1)$ from each of their viability specialist neighbors.
 290 But how many of their neighbors are viability specialists? We label the fraction of cells connected to
 291 fecundity specialists that are viability specialists f , i.e., f is the mean number of viability specialists
 292 connected to each fecundity specialist divided by z , averaged over all fecundity specialists. For a
 293 bipartite graph, $f = 1$; for a randomly connected graph on which half of cells are viability specialists
 294 and half of cells are fecundity specialists, $f = 1/2$. Group fitness is thus:

$$W_S = \frac{zfN}{2(z+1)}. \quad (2)$$

295 Here, $zf/(z + 1)$ is the average viability returns each fecundity specialist has received after sharing,
 296 which is multiplied by the amount of fecundity each fecundity specialist has (1) and the number of
 297 fecundity specialists ($N/2$). Writing W_S in terms of W_G :

$$W_S = \frac{2zfW_G}{z+1}. \quad (3)$$

298 Specialists will be favored if the ratio $W_S/W_G > 1$. This will be true if:

$$f > \frac{z+1}{2z}, \quad (4)$$

299 which reduces to:

$$f > \frac{1}{2} + \frac{1}{2z}. \quad (5)$$

300 This inequality implies that specialization will only be favored if fecundity specialists are preferen-
 301 tially connected to viability specialists, i.e., if $f > 1/2$. Further, for a fully connected network $f = 1/2$,
 302 so this inequality is never satisfied, i.e., specialists cannot have larger fitness than generalists for
 303 $\alpha = 1$ and fully connected topologies, as classically predicted.

304 Further, f cannot be more than 1, so if the threshold from the inequality in Eq. 5 is greater
 305 than or equal to 1, specialization cannot be favored for $\alpha < 1$. Thus, specialization for $\alpha < 1$ is only
 306 possible if:

$$\frac{1}{2} + \frac{1}{2z} < 1, \quad (6)$$

307 which reduces to: $z > 1$. This again reproduces a classic result: specialization for $\alpha < 1$ is not possible
 308 for disconnected cells.

309 This analysis allows us to interrogate specific cases. For example, if $z = 3$, f must be greater than
 310 $2/3$, while if $z = 4$, f must only be greater than $5/8$. Can such networks be constructed? The answer
 311 will depend on both the number of cells and how they are connected. Ultimately, the question of if
 312 a graph can be made with particular values of f and z is a graph coloring problem, and beyond the
 313 scope of this manuscript. However, this inequality presents a useful heuristic which can be used to
 314 determine if specialization is favored by measuring just a few properties of the graph.

315 Effect of varying ratios of specialists

316 We now allow the fraction of fecundity specialists to be X (rather than forcing $X = 1/2$). For
317 generalists, the group fitness is unchanged, $W_G = N/4$, while for specialists the group fitness is:

$$W_S = \frac{zfXN}{z+1}. \quad (7)$$

318 Writing W_S in terms of W_G gives:

$$W_S = \frac{4zfXW_G}{z+1}. \quad (8)$$

319 Specialists will be favored if the ratio $W_S/W_G > 1$. This will be true if:

$$f > \frac{z+1}{4Xz} = \frac{1}{4X} + \frac{1}{4Xz}. \quad (9)$$

320 Compared to the threshold value of f when $X = 1/2$, if $X > 1/2$, i.e., more than half of cells are
321 fecundity specialists, the value of f necessary for specialization to be favored is lower. If $X < 1/2$,
322 the threshold value of f is higher than if $X = 1/2$. In other words, 1:2 is different from 2:1, and
323 they both are different from 1:1. Once again, the question of if a particular configuration can be
324 created—and how—is a graph coloring problem beyond the scope of this manuscript. However, this
325 mean field heuristic gives us some information about how to expect graphs with different ratios of
326 specialists to generalists to behave.

327 We again ask what must be true for f to be less than 1 (if $f > 1$, specialization will not be
328 favored). Thus, specialization is only possible if:

$$\frac{1}{4X} + \frac{1}{4Xz} < 1, \quad (10)$$

329 which reduces to:

$$X > \frac{1}{4} + \frac{1}{4z}. \quad (11)$$

330 For a mean field model, specialization with $\alpha < 1$ is impossible if fewer than one fourth of cells are
331 fecundity specialists. We stress here that this is a mean field model, and does not apply to scenarios
332 in which cells have a wide range of values of z . If such networks do or do not favor specialization
333 for $\alpha < 1$ will again be a graph coloring problem.

334 Discussion

335 During the evolution of multicellularity, formerly autonomous unicellular organisms evolve into
336 functionally-integrated parts of a new higher-level organism *West et al. (2015); Michod and Nedelcu*
337 *(2003)*. Evolutionary game theory *Corning and Szathmary (2015); Nash (1950); Smith (1988)* argues
338 that functional specialization should only evolve when increased investment in trade increases
339 reproductive output. Conventionally, this requires returns from specialization to be accelerating, i.e.,
340 convex or super-linear *Szathmary and Smith (1995); Smith and Szathmary (1997); Goldsby et al.*
341 *(2012); Corning and Szathmary (2015); Boza et al. (2014); Taborsky et al. (2016); Page et al. (2006);*
342 *Rueffler et al. (2012); Szekely et al. (2013)*. While this idea is intuitive, it is, in the case of fixed
343 group topology, also overly restrictive. In this paper, we explore how social interactions within
344 groups, measured by their network topology, affect the evolution of reproductive specialization.
345 Indeed, when all cells within groups interact (with equal interaction strength), returns on investment
346 must be an accelerating, i.e., convex, function of investment for specialization to evolve (figure 1a)
347 *Szathmary and Smith (1995); Smith and Szathmary (1997); Corning and Szathmary (2015); Cooper*
348 *and West (2018)*. Yet for a broad class of sparsely-connected networks, complete specialization
349 can evolve even when the viability and fecundity return on investment curves are saturating, i.e.,
350 concave (figure 3).

351 To understand how specialization can be favored despite concave return on investment (ROI)
 352 curves, consider Jensen's inequality. Jensen's inequality states that for a convex function $F(x)$,
 353 $\langle F(x) \rangle > F(\langle x \rangle)$, i.e., the average value of $F(x)$, $\langle F(x) \rangle$, is larger than $F(\langle x \rangle)$, where $\langle x \rangle$ is the average
 354 value of x . A corollary of Jensen's inequality is that the opposite is true for concave functions,
 355 i.e., for a concave function $G(x)$, $\langle G(x) \rangle < G(\langle x \rangle)$. Jensen's inequality guarantees that for concave
 356 ROI functions generalists produce more total viability and fecundity than specialists, and that for
 357 convex ROI functions specialists produce more total viability and fecundity than generalists. For
 358 fully connected topologies and symmetric sharing, an increase in absolute productivity is directly
 359 translated into an increase in group fitness.

360 Crucially, however, the connection between ROI convexity/concavity and fitness is indirect.
 361 Jensen's inequality directly relates the degree of specialization to the average v and average b , but
 362 does not itself say anything about average vb and group fitness. For fully connected topologies
 363 and symmetric sharing, average vb happens to be directly proportional to average v and average b ;
 364 combined with Jensen's inequality, this fact allows one to connect the degree of specialization to
 365 group fitness.

366 That Jensen's inequality connects the degree of specialization to average v and average b , but
 367 not group fitness is a crucial distinction. Jensen's inequality is a mathematical rule truism, and
 368 cannot be violated. Indeed, for any concave ROI function, generalists will produce more v and b
 369 than specialists, regardless of topology or if sharing is symmetric or asymmetric. This fact is just
 370 as true for sparse topologies and asymmetric sharing as it is for fully connected topologies and
 371 symmetric sharing. However, for sparse topologies and asymmetric sharing, average vb is not
 372 directly proportional to average v and average b , but instead strongly depends on network structure.
 373 With asymmetric sharing and sparse topologies, Jensen's inequality still informs the average viability
 374 and fecundity produced, but does not directly inform the group fitness.

375 Rather than being unusual, networks favoring specialization readily arise as a consequence of
 376 physical processes structuring simple cellular groups *Allen et al. (2017)*. For example, septin defects
 377 during cell division create multicellular groups with simple graph structures (Figure 4 a and b), where
 378 cells are connected only to parents and offspring *Bengtson et al. (2017b)*; *Droser and Gehling (2008)*;
 379 *Ratcliff et al. (2012, 2013)*. If cells share resources only with physically-attached neighbors, then
 380 the physical topology of the group describes its interaction topology, and these sparse networks
 381 strongly favor reproductive specialization. Finally, we note that the primary benefit of sparsity is
 382 that sparse networks are likely to be at least somewhat bipartite. The more bipartite-like a network
 383 is, the less effort is wasted, and the easier it is for specialization to be favored.

384 Disentangling the evolutionary underpinnings of ancient events is notoriously difficult. Still, it is
 385 worth examining the independent origins of complex multicellularity, which are independent runs
 386 of parallel natural experiments in extreme sociality. Complex multicellularity (large multicellular
 387 organisms with considerable cellular differentiation) has evolved in at least 5 eukaryotic lineages,
 388 once each in the animals *King (2004)*, land plants *Kenrick and Crane (1997)*, and brown algae
 389 *Silberfeld et al. (2010)*, two or three times in the red algae *Cock and Collén (2015)*; *Yoon et al. (2006)*,
 390 and 8-11 times in fungi *Nagy et al. (2018)*. In all cases other than animals, these organisms form
 391 multicellular bodies via permanent cell-cell bonds, creating long-lasting highly structured cellular
 392 networks. Both fossil and phylogenetic evidence suggests that early multicellular organisms in these
 393 lineages were considerably less complex, growing as relatively simple graph structures. For example,
 394 1.2 billion year old red algae formed linear filaments of cells *Butterfield (2000b)*, basal multicellular
 395 charophyte algae formed circular sheets of cells radiating from a common center *Kenrick and*
 396 *Crane (1997)*, the ancestor of the brown algae likely formed a branched haplostichous thallus that
 397 was either filamentous or pseudoparenchymatous *Silberfeld et al. (2010)*, and hyphal fungi are
 398 primarily composed of linear chains of cells. Much less is known about the topology of animals
 399 prior to the evolution of cellular specialization. One hypothesis is that early metazoans resembled
 400 extant colonial choanoflagellates *Fairclough et al. (2013)*, the closest-living protistan relatives of the
 401 animals *Fairclough et al. (2010)*. Extant colony-forming choanoflagellates have evolved a variety of

402 multicellular structures with sparse cellular topologies and permanent cell-cell bonds. For example,
 403 many species form branched, tree-like structures *Boenigk (2015)*, *Choanoeca flexa* grows as a sheet of
 404 cells *Brunet et al. (2019)*, and *Salpingoceca rosetta* can form either linear chains or rosettes in which
 405 the cells are connected via cytoplasmic bridges formed through incomplete cytokinesis *Dayel et al.*
 406 *(2011)*. While these growth forms are quite diverse, they all share characteristics (i.e., permanent
 407 cellular bonds and sparse topologies) that promote the evolution of cellular differentiation.

408 The main differences between our work and previous investigations of the effect of group
 409 topology on specialization is that we consider the productivity of groups as a whole, not the cells
 410 within them, and we consider situations of highly asymmetric sharing. Our approach is general,
 411 and can be applied to other systems of trade and specialization, so long as 1) only the aggregate
 412 productivity of the group (and not the particles within it) is maximized, 2) the productivity of each
 413 particle within the group is a multiplicative function of returns on investment into two (or more)
 414 tasks, and 3) there is an asymmetry in how products of those investments are shared. While in this
 415 work we have focused on reproductive division of labor, a process in which fecundity returns are
 416 not shared at all, we show in the supplement that as long as sharing of two goods is sufficiently
 417 asymmetric, specialization with saturating returns on investment can still be adaptive (Supplemental
 418 Figure 2).

419 Finally, we note that alternative paths to specialization likely exist. For example, cells at differ-
 420 ent positions in a group may experience different local environments, which may produce cells
 421 with varied fecundity-viability trade-offs. A previous paper demonstrated that the evolution of
 422 specialization is favored if these ‘positional effects’ result in an initially heterogeneous population of
 423 cell types *Tverskoi et al. (2018)*. However, these positional effects were considered for the case of
 424 well-mixed groups (i.e., completely connected network topologies). We thus anticipate that future
 425 work examining the relationship between cellular interaction topology and cellular heterogeneity
 426 (as well as a wide range of complex and varied relationships between viability, fecundity, and
 427 multicellular fitness) will provide unique insight into the origin and diversity of multicellular forms.

428 Conclusion

429 We explored the evolution of reproductive specialization in multicellular groups with various cellular
 430 interaction topologies. Our results demonstrate that group topological structure can play a key role
 431 in the evolution of reproductive division of labor. Indeed, within a broad class of sparsely connected
 432 networks, specialization is favored even when the returns from cooperation are saturating (i.e.,
 433 concave); this result is in direct contrast to the prevailing view that accelerating (i.e., convex), returns
 434 are required for natural selection to favor increased specialization *Cooper and West (2018)*; *Michod*
 435 *et al. (2006)*; *Ispolatov et al. (2012)*; *Solari et al. (2013)*; *Michod (2007)*; *West et al. (2015)*. Our
 436 results underscore the central importance of life history trade-offs in the origin of reproductive
 437 specialization *Michod et al. (2006)*; *Michod (2007)*; *Hammerschmidt et al. (2014)*; *van Gestel and*
 438 *Tarnita (2017)*; *Noh et al. (2018)*, and support the emerging consensus that evolutionary transitions
 439 in individuality are not necessarily highly constrained *Ratcliff et al. (2012, 2017)*; *Fairclough et al.*
 440 *(2010)*; *Brunet and King (2017)*; *Pennisi (2018)*; *Black et al. (2019)*; *Rose et al. (2019)*; *van Gestel and*
 441 *Tarnita (2017)*; *Black et al. (2019)*; *Staps et al. (2019)*; *Grosberg and Strathmann (2007)*.

442 Methods

443 Analysis

444 The gradient of the fitness with respect to the group investment strategy \vec{v} , is

$$\frac{\partial W}{\partial \vec{v}} = \sum_{k=1}^N \hat{e}_k \alpha \left(v_k^{\alpha-1} \sum_{j=1}^N c_{kj} (1 - v_j)^\alpha - (1 - v_k)^{\alpha-1} \sum_{j=1}^N c_{jk} v_j^\alpha \right) \quad (12)$$

445 where \hat{e}_k is a unit vector in the k^{th} direction. First notice that if $\mathbf{c} = \mathbf{c}^T$, and $\vec{v} = \frac{1}{2}\vec{\mathbb{1}}$ where $\vec{\mathbb{1}}$ is a vector
 446 of ones, then the gradient is zero. This strategy, $\vec{v} = \frac{1}{2}\vec{\mathbb{1}}$, corresponds to the ‘generalist’ approach,
 447 where every cell invests equally into both tasks. Call it the generalist strategy. Second, notice that
 448 if $\mathbf{c} \neq \mathbf{c}^T$ then the gradient is *not* zero under the generalist strategy, so at least some degree of
 449 specialization must be necessary to maximize fitness. To determine the stability of this solution we
 450 examine \mathbf{H}^* , the Hessian (see SI eq. 3) evaluated at the generalist critical point. If \mathbf{H}^* is negative
 451 definite, then the generalist strategy is a fitness maximum and is therefore an optimal strategy. If,
 452 on the other hand, \mathbf{H}^* has both positive and negative eigenvalues then the generalist strategy lies at
 453 a saddle point within the fitness landscape, and therefore the optimal strategy must be somewhere
 454 else in (or on the boundary of) the domain (i.e. $v_i \in [0, 1]$ for all $i \in \{1, 2, \dots, N\}$). Finally, note that \mathbf{H}^* is
 455 never positive definite since $\vec{\mathbb{1}}$ is always an eigenvector with negative eigenvalue (when $\mathbf{c} = \mathbf{c}^T$).

456 We also use the zero crossing of the largest eigenvalue of \mathbf{H}^* evaluated at $\vec{v} = \frac{1}{2}\vec{\mathbb{1}}$ and $\beta = 1$ as an
 457 overall measure of how amenable a network is to specialization, even when $\mathbf{c} \neq \mathbf{c}^T$.

458 Evolutionary simulations

459 Our evolutionary simulations maintain the same overall structure as the Wright-Fisher model:
 460 a discrete-time Markov chain framework with fitness-weighted multinomial sampling between
 461 generations and constant population size. Therefore we refer to them as Wright-Fisher evolutionary
 462 simulations. We initialize a population of $\mathcal{N} = 1000$ groups, each of group size $N = 10$, with uniform
 463 random investment strategies. We then let them evolve for 1000 generations, selecting offspring
 464 according to the relative fitness of each group (see eq. 1). At each generation there is a 2% chance
 465 for a mutation to a given group’s investment strategy \vec{v} . If a mutation occurs, a new investment
 466 strategy is selected from a truncated multivariate gaussian distribution centered at the current
 467 (pre-mutation) investment strategy and with standard deviation equal to $\frac{1}{10}\vec{v}$. After mutations each
 468 group’s fitness is calculated according to eq. 1, and the population is ranked according to fitness.
 469 Finally, \mathcal{N} groups are selected (with replacement) to populate the next generation, according to a
 470 multinomial distribution weighted by the groups’ fitness ranks.

471 Measuring specialization

472 To quantify the degree of specialization associated with a given group’s optimal investment strategy—
 473 the one which maximizes the fitness— we introduce the following metric, which we refer to simply
 474 as “Specialization”:

$$S = \frac{2}{N} \sum_{i=1}^N \left(\max(v_i, 1 - v_i) - \frac{1}{2} \right). \quad (13)$$

475 Specialization ranges from 0 (for groups consisting of cells investing equally in functions v and b) to
 476 1 (for groups consisting of cells investing exclusively in either function

477 Code availability

478 All evolutionary simulations and other computations associated with this work are available at
 479 github.com/dyanni3/topologicalConstraintsSpecialization.

480 References

- 481 Allen, B., Lippner, G., Chen, Y.-T., Fotouhi, B., Momeni, N., Yau, S.-T., and Nowak, M. A. (2017). Evolutionary
 482 dynamics on any population structure. *Nature*, 544:227 EP –.
- 483 Amado, A., Batista, C., and Campos, P. R. (2018). A theoretical approach to the size-complexity rule. *Evolution*,
 484 72(1):18–29.
- 485 Bengtson, S., Rasmussen, B., Ivarsson, M., Muhling, J., Broman, C., Marone, F., Stampanoni, M., and Bekker, A.
 486 (2017a). Fungus-like mycelial fossils in 2.4-billion-year-old vesicular basalt. *Nature Ecology & Evolution*,
 487 1:0141 EP –. Article.

- 488 Bengtson, S., Sallstedt, T., Belivanova, V., and Whitehouse, M. (2017b). Three-dimensional preservation of cellular
489 and subcellular structures suggests 1.6 billion-year-old crown-group red algae. *PLoS Biology*, 15(3):1–38.
- 490 Berman-Frank, I., Quigg, A., Finkel, Z. V., Irwin, A. J., and Haramaty, L. (2007). Nitrogen-fixation strategies and fe
491 requirements in cyanobacteria. *Limnology and Oceanography*, 52(5):2260–2269.
- 492 Black, A. J., Bourrat, P., and Rainey, P. B. (2019). Ecological scaffolding and the evolution of individuality: the
493 transition from cells to multicellular life. *BioRxiv*, page 656660.
- 494 Boenigk, J. (2015). The choanoflagellates: evolution, biology and ecology.
- 495 Bonner, J. T. (1998). The origins of multicellularity. *Integrative Biology: Issues, News, and Reviews*, 1(1):27–36.
- 496 Boza, G., Szilágyi, A., Kun, Á., Santos, M., and Szathmáry, E. (2014). Evolution of the division of labor between
497 genes and enzymes in the rna world. *PLOS Computational Biology*, 10(12):1–9.
- 498 Brunet, T. and King, N. (2017). The origin of animal multicellularity and cell differentiation. *Developmental Cell*,
499 43(2):124–140.
- 500 Brunet, T., Larson, B. T., Linden, T. A., Vermeij, M. J. A., McDonald, K., and King, N. (2019). Light-regulated collective
501 contractility in a multicellular choanoflagellate. *Science*, 366(6463):326–334.
- 502 Buss, L. W. (1988). *The Evolution of Individuality*. Princeton University Press.
- 503 Butterfield, N. J. (2000a). *Bangiomorpha pubescens* n. gen., n. sp.: implications for the evolution of sex,
504 multicellularity, and the mesoproterozoic/neoproterozoic radiation of eukaryotes. *Paleobiology*, 26(3):386–
505 404.
- 506 Butterfield, N. J. (2000b). *Bangiomorpha pubescens* n. gen., n. sp.: implications for the evolution of sex,
507 multicellularity, and the mesoproterozoic/neoproterozoic radiation of eukaryotes. *Paleobiology*, 26(3).
- 508 Cavalier-Smith, T. (2017). Origin of animal multicellularity: precursors, causes, consequences—the choanoflag-
509 ellate/sponge transition, neurogenesis and the cambrian explosion. *Philosophical Transactions of the Royal
510 Society of London B: Biological Sciences*, 372(1713).
- 511 Claessen, D., Rozen, D. E., Kuipers, O. P., Søgaard-Andersen, L., and Van Wezel, G. P. (2014). Bacterial solutions to
512 multicellularity: a tale of biofilms, filaments and fruiting bodies. *Nature Reviews Microbiology*, 12(2):115–124.
- 513 Cock, J. M. and Collén, J. (2015). Independent emergence of complex multicellularity in the brown and red algae.
514 In *Evolutionary Transitions to Multicellular Life*, pages 335–361. Springer.
- 515 Cooper, G. A. and West, S. A. (2018). Division of labour and the evolution of extreme specialization. *Nature
516 Ecology & Evolution*.
- 517 Corning, P. A. and Szathmáry, E. (2015). Synergistic selection: A darwinian frame for the evolution of complexity.
518 *Journal of Theoretical Biology*, 371:45 – 58.
- 519 Dayel, M. J., Alegado, R. A., Fairclough, S. R., Levin, T. C., Nichols, S. A., McDonald, K., and King, N. (2011). Cell
520 differentiation and morphogenesis in the colony-forming choanoflagellate salpingoeca rosetta. *Developmental
521 biology*, 357(1):73–82.
- 522 Droser, M. L. and Gehling, J. G. (2008). Synchronous aggregate growth in an abundant new ediacaran tubular
523 organism. *Science*, 319(5870):1660–1662.
- 524 Fairclough, S. R., Chen, Z., Kramer, E., Zeng, Q., Young, S., Robertson, H. M., Begovic, E., Richter, D. J., Russ, C.,
525 Westbrook, M. J., et al. (2013). Premetazoan genome evolution and the regulation of cell differentiation in the
526 choanoflagellate salpingoeca rosetta. *Genome biology*, 14(2):R15.
- 527 Fairclough, S. R., Dayel, M. J., and King, N. (2010). Multicellular development in a choanoflagellate. *Current biology
528 : CB*, 20(20):R875–R876.
- 529 Findlay, R. (2008). Comparative advantage. *The New Palgrave Dictionary of Economics: Volume 1–8*, pages 924–929.
- 530 Folse III, H. J. and Roughgarden, J. (2010). What is an individual organism? a multilevel selection perspective. *The
531 Quarterly review of biology*, 85(4):447–472.
- 532 Goldsby, H. J., Dornhaus, A., Kerr, B., and Ofria, C. (2012). Task-switching costs promote the evolution of division
533 of labor and shifts in individuality. *Proceedings of the National Academy of Sciences*, 109(34):13686–13691.

- 534 Grosberg, R. K. and Strathmann, R. R. (2007). The evolution of multicellularity: A minor major transition? *Annual*
535 *Review of Ecology, Evolution, and Systematics*, 38:621–654.
- 536 Hammerschmidt, K., Rose, C. J., Kerr, B., and Rainey, P. B. (2014). Life cycles, fitness decoupling and the evolution
537 of multicellularity. *Nature*, 515(7525):75.
- 538 Heim, N. A., Payne, J. L., Finnegan, S., Knope, M. L., Kowalewski, M., Lyons, S. K., McShea, D. W., Novack-Gottshall,
539 P. M., Smith, F. A., and Wang, S. C. (2017). Hierarchical complexity and the size limits of life. *Proceedings of the*
540 *Royal Society of London B: Biological Sciences*, 284(1857).
- 541 Hidalgo, C. A. and Hausmann, R. (2009). The building blocks of economic complexity. *Proceedings of the National*
542 *Academy of Sciences*, 106(26):10570–10575.
- 543 Ispolatov, I., Ackermann, M., and Doebeli, M. (2012). Division of labour and the evolution of multicellularity.
544 *Proceedings of the Royal Society of London B: Biological Sciences*, 279(1734):1768–1776.
- 545 Kenrick, P. and Crane, P. R. (1997). The origin and early evolution of plants on land. *NATURE*, 389:4.
- 546 King, N. (2004). The unicellular ancestry of animal development. *Developmental cell*, 7(3):313–325.
- 547 Kirk, D. L. (2005a). A twelve-step program for evolving multicellularity and a division of labor. *BioEssays*,
548 27(3):299–310.
- 549 Kirk, D. L. (2005b). A twelve-step program for evolving multicellularity and a division of labor. *BioEssays*,
550 27(3):299–310.
- 551 Knoll, A. H. (2011). The multiple origins of complex multicellularity. *Annual Review of Earth and Planetary Sciences*,
552 39:217–239.
- 553 Libby, E. and Ratcliff, W. C. (2014). Ratcheting the evolution of multicellularity. *Science*, 346(6208):426–427.
- 554 Lieberman, E., Hauert, C., and Nowak, M. A. (2005). Evolutionary dynamics on graphs. *Nature*, 433(7023):312.
- 555 McCarthy, M. and Enquist, B. (2005). Organismal size, metabolism and the evolution of complexity in metazoans.
556 In *Evolutionary Ecology Research*, volume 7, pages 681–696.
- 557 McClain, C. R. and Boyer, A. G. (2009). Biodiversity and body size are linked across metazoans. *Proceedings of the*
558 *Royal Society of London B: Biological Sciences*, 276(1665):2209–2215.
- 559 McShea, D. W. (2000). Functional complexity in organisms: Parts as proxies. *Biology and Philosophy*, 15(5):641–
560 668.
- 561 Michod, R. E. (1999). Darwinian dynamics: Evolutionary transitions in fitness and individuality. *Complexity*,
562 5(1):42–43.
- 563 Michod, R. E. (2005). On the transfer of fitness from the cell to the multicellular organism. *Biology and Philosophy*,
564 20(5):967–987.
- 565 Michod, R. E. (2007). Evolution of individuality during the transition from unicellular to multicellular life.
566 *Proceedings of the National Academy of Sciences of the United States of America*, 104(Suppl 1):8613–8618.
- 567 Michod, R. E. and Nedelcu, A. M. (2003). On the reorganization of fitness during evolutionary transitions in
568 individuality. *Integrative and Comparative Biology*, 43(1):64–73.
- 569 Michod, R. E. and Roze, D. (1997). Transitions in individuality. *Proceedings of the Royal Society of London B:*
570 *Biological Sciences*, 264(1383):853–857.
- 571 Michod, R. E., Viossat, Y., Solari, C. A., Hurand, M., and Nedelcu, A. M. (2006). Life-history evolution and the origin
572 of multicellularity. *Journal of Theoretical Biology*, 239(2):257 – 272. Special Issue in Memory of John Maynard
573 Smith.
- 574 Nagy, L. G., Kovács, G. M., and Krizsán, K. (2018). Complex multicellularity in fungi: evolutionary convergence,
575 single origin, or both? *Biological Reviews*, 93(4):1778–1794.
- 576 Nash, J. F. (1950). Equilibrium points in n-person games. *Proceedings of the National Academy of Sciences*,
577 36(1):48–49.

- 578 Noh, S., Geist, K. S., Tian, X., Strassmann, J. E., and Queller, D. C. (2018). Genetic signatures of microbial altruism
579 and cheating in social amoebas in the wild. *Proceedings of the National Academy of Sciences*, 115(12):3096–3101.
- 580 Page, R. E., Scheiner, R., Erber, J., and Amdam, G. V. (2006). The development and evolution of division of labor
581 and foraging specialization in a social insect (apis mellifera l.). *Current Topics in Developmental Biology*, 74:253 –
582 286.
- 583 Pavlogiannis, A., Tkadlec, J., Chatterjee, K., and Nowak, M. A. (2018). Construction of arbitrarily strong amplifiers
584 of natural selection using evolutionary graph theory. *Communications Biology*, 1(1):71.
- 585 Pennisi, E. (2018). The power of many. *Science*, 360(6396):1388–1391.
- 586 Queller, D. C. and Strassmann, J. E. (2009). Beyond society: the evolution of organismality. *Philosophical
587 Transactions of the Royal Society of London B: Biological Sciences*, 364(1533):3143–3155.
- 588 Ratcliff, W. C., Denison, R. F., Borrello, M., and Travisano, M. (2012). Experimental evolution of multicellularity.
589 *Proceedings of the National Academy of Sciences*, 109(5):201115323–1600.
- 590 Ratcliff, W. C., Fankhauser, J. D., Rogers, D. W., Greig, D., and Travisano, M. (2015). Origins of multicellular
591 evolvability in snowflake yeast. *Nature Communications*, 6:6102+.
- 592 Ratcliff, W. C., Herron, M., Conlin, P. L., and Libby, E. (2017). Nascent life cycles and the emergence of higher-level
593 individuality. *Phil. Trans. R. Soc. B*, 372(1735):20160420.
- 594 Ratcliff, W. C., Pentz, J. T., and Travisano, M. (2013). Tempo and mode of multicellular adaptation in experimentally
595 evolved *Saccharomyces cerevisiae*. *Evolution*, 67(6):1573–1581.
- 596 Rose, C. J., Hammerschmidt, K., and Rainey, P. B. (2019). Meta-population structure and the evolutionary
597 transition to multicellularity.
- 598 Rueffler, C., Hermisson, J., and Wagner, G. P. (2012). Evolution of functional specialization and division of labor.
599 *Proceedings of the National Academy of Sciences*, 109(6):1830–1831.
- 600 Silberfeld, T., Leigh, J. W., Verbruggen, H., Cruaud, C., De Reviers, B., and Rousseau, F. (2010). A multi-locus
601 time-calibrated phylogeny of the brown algae (heterokonta, ochrophyta, phaeophyceae): Investigating the
602 evolutionary nature of the “brown algal crown radiation”. *Molecular phylogenetics and evolution*, 56(2):659–674.
- 603 Smith, J. and Szathmáry, E. (1997). *The Major Transitions in Evolution*. OUP Oxford.
- 604 Smith, J. M. (1988). *Evolution and the Theory of Games*, pages 202–215. Springer US, Boston, MA.
- 605 Solari, C. A., Kessler, J. O., and Goldstein, R. E. (2013). A general allometric and life-history model for cellular
606 differentiation in the transition to multicellularity. *The American Naturalist*, 181(3):369–380. PMID: 23448886.
- 607 Staps, M., van Gestel, J., and Tarnita, C. E. (2019). Emergence of diverse life cycles and life histories at the origin
608 of multicellularity. *Nature ecology & evolution*, 3(8):1197–1205.
- 609 Szathmáry, E. and Smith, J. M. (1995). The major evolutionary transitions. *Nature*, 374(6519):227–232.
- 610 Szekely, P., Sheftel, H., Mayo, A., and Alon, U. (2013). Evolutionary tradeoffs between economy and effectiveness
611 in biological homeostasis systems. *PLOS Computational Biology*, 9(8):1–14.
- 612 Taborsky, M., Frommen, J. G., and Riehl, C. (2016). Correlated pay-offs are key to cooperation. *Philosophical
613 Transactions of the Royal Society of London B: Biological Sciences*, 371(1687).
- 614 Tverskoi, D., Makarenkov, V., and Aleskerov, F. (2018). Modeling functional specialization of a cell colony under
615 different fecundity and viability rates and resource constraint. *PloS one*, 13(8):e0201446.
- 616 Umen, J. G. (2014). Green algae and the origins of multicellularity in the plant kingdom. *Cold Spring Harbor
617 perspectives in biology*, 6(11):a016170.
- 618 van Gestel, J. and Tarnita, C. E. (2017). On the origin of biological construction, with a focus on multicellularity.
619 *Proceedings of the National Academy of Sciences*, 114(42):11018–11026.
- 620 West, S. A., Fisher, R. M., Gardner, A., and Kiers, E. T. (2015). Major evolutionary transitions in individuality.
621 *Proceedings of the National Academy of Sciences*, 112(33):10112–10119.

- 622 Wey, T., Blumstein, D. T., Shen, W., and Jordan, F. (2008). Social network analysis of animal behaviour: a promising
623 tool for the study of sociality. *Animal behaviour*, 75(2):333–344.
- 624 Willensdorfer, M. (2008). Organism size promotes the evolution of specialized cells in multicellular digital
625 organisms. *Journal of evolutionary biology*, 21(1):104–110.
- 626 Yoon, H. S., Müller, K. M., Sheath, R. G., Ott, F. D., and Bhattacharya, D. (2006). Defining the major lineages of red
627 algae (rhodophyta) 1. *Journal of phycology*, 42(2):482–492.